A Mode-Matching Technique for the Analysis of Waveguide-on-Substrate Components

Jan Schorer and Jens Bornemann

Department of Electrical and Computer Engineering, University of Victoria, Victoria, BC, V8W 2Y2 Canada

***Abstract* — The mode-matching technique (MMT) is employed to analyze the transition from substrate integrated waveguide (SIW) to an empty waveguide that is mounted on top of the substrate. Coupling between the two layers is facilitated by an aperture of the thickness of the substrate's metallization. By appropriately segmenting the transition, a simple and fast MMT routine is developed. Results obtained for a single waveguide resonator mounted on the substrate agree well with simulations in CST and HFSS and thus validate the MMT code. It is expected that this model will aid in the design of substrate mounted waveguide (SMW) filters.**

***Index Terms* — Substrate integrated waveguide, substrate mounted waveguide filter, mode-matching technique.**

I. Introduction

Substrate integrated circuits (SICs) provide a convenient opportunity for integration of previously bulky components in single- or multilayered substrate arrangements. Especially substrate integrated waveguide (SIW) circuitry has been developed into a mature technology over the last decade [1].

In order to interface with surface mounted, active components, interconnects to other transmission line structures, such as microstrip or coplanar waveguide, are required [2]. To reduce the relatively high losses in microstrip filters operating in the higher GHz range, a substrate mounted waveguide (SMW) principle has been introduced [3]. A Ka-band prototype demonstrates lower insertion loss and electrical performance that could not be obtained with a planar filter structure [4]. Due to the fact that SIW filter and diplexer technologies suffer from relatively high insertion losses, the SMW principle lends itself to applications in SIW.

Therefore, this paper focuses on a transition from SIW to SMW and presents an MMT approach to design such an interface. It is expected that this model will aid in the full-wave design of SMW waveguide filters and diplexers and thus contribute to the solution of a bottleneck in SIW technology.

II. Theory

Fig. 1 shows a sketch of the SIW-to-SMW transition. The SIW is coupled to the SMW by an aperture in the top metallization of the substrate. A certain distance after the aperture, the SIW is shorted using a row of via holes. In the waveguide, the fundamental TE_{10} mode is excited, and the distance to the short is adjusted to improve the transmission.

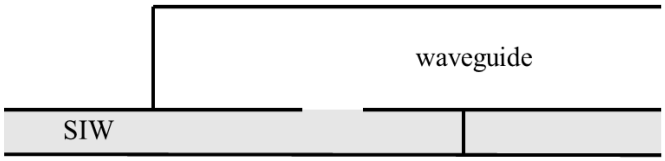

Fig. 1. Side view of the transition between SIW and substrate mounted waveguide (SMW).

The segmentation involved in the MMT is shown in Fig. 2 and involves discontinuities in all three directions. Note that the subsections are either homogeneously filled with the dielectric material of the substrate (or with air) or are entirely transverse to the discontinuities. Therefore, no hybrid modes but a full set of TE_{mn} and TM_{mn} modes need to be considered.

Referring to Fig. 2, the transverse electric and magnetic fields in regions I and II at their respective boundaries with region IV are given as:

$$\begin{aligned}
\vec{E}_T^I(z=0) = &\sum_q \sqrt{Z_{hq}^I}\left(\nabla T_{hq}^I \times \vec{e}_z\right)\left[F_{hq}^I + B_{hq}^I\right] \\
&- \sum_p \sqrt{Z_{ep}^I}\left(\nabla T_{ep}^I\right)\left[F_{ep}^I + B_{ep}^I\right] = \vec{E}_T^{II}(z=c) \\
\vec{H}_T^I(z=0) = &\sum_q \sqrt{Y_{hq}^I}\left(\nabla T_{hq}^I\right)\left[F_{hq}^I - B_{hq}^I\right] \\
&+ \sum_p \sqrt{Y_{ep}^I}\left(\nabla T_{ep}^I \times \vec{e}_z\right)\left[F_{ep}^I - B_{ep}^I\right] \\
&= \vec{H}_T^{II}(z=c)
\end{aligned} \tag{1}$$

In (1), q and p are mode indices defining the cross-section functions as:

$$\begin{aligned}
T_{hq\to m,n}^I &= A_q^I \frac{\cos\left(\frac{m\pi}{a}x\right)}{\sqrt{1+\delta_{0m}}} \frac{\cos\left(\frac{n\pi}{b}y\right)}{\sqrt{1+\delta_{0n}}} = T_{hq}^{II} \\
T_{ep\to m,n}^I &= D_p^I \sin\left(\frac{m\pi}{a}x\right)\sin\left(\frac{n\pi}{b}y\right) = T_{ep}^{II}
\end{aligned} \tag{2}$$

A and D are normalization terms, and δ is the Kronecker delta. Parameter a in (2) denotes the equivalent SIW width [5].
F and B in (1) are forward and backward propagating (or evanescent) wave amplitudes, respectively, and wave impedances and admittances are given as:

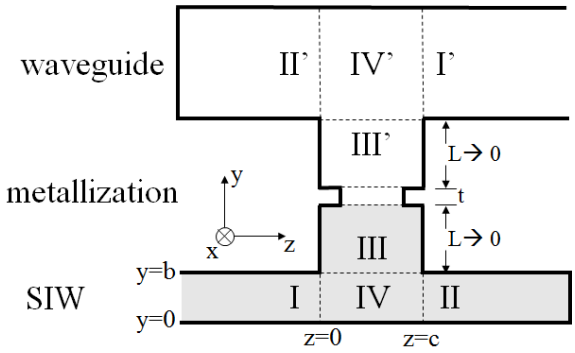

Fig. 2. Segmentation of the SIW-to-SMW transition for MMT analysis.

$$Z^I_{hq\to m,n} = \frac{1}{Y^I_{hq}} = \frac{\omega\mu_0}{\sqrt{k_0^2\varepsilon_r - \left(\frac{m\pi}{a}\right)^2 - \left(\frac{n\pi}{b}\right)^2}}$$

$$Y^I_{ep\to m,n} = \frac{1}{Z^I_{ep}} = \frac{\omega\varepsilon_0\varepsilon_r}{\sqrt{k_0^2\varepsilon_r - \left(\frac{m\pi}{a}\right)^2 - \left(\frac{n\pi}{b}\right)^2}} \tag{3}$$

The respective fields and quantities of region III at its boundary region IV are:

$$\begin{aligned}\vec{E}^{III}_T(y=b) = &\sum_r \sqrt{Z^{III}_{hr}}\left(\nabla T^{III}_{hr}\times\vec{e}_y\right)\left[F^{III}_{hr} + B^{III}_{hr}\right] \\ &-\sum_s \sqrt{Z^{III}_{es}}\left(\nabla T^{III}_{es}\right)\left[F^{III}_{es} + B^{III}_{es}\right] \\ \vec{H}^{III}_T(y=b) = &\sum_r \sqrt{Y^{III}_{hr}}\left(\nabla T^{III}_{hr}\right)\left[F^{III}_{hr} - B^{III}_{hr}\right] \\ &+\sum_s \sqrt{Y^{III}_{es}}\left(\nabla T^{I}_{es}\times\vec{e}_y\right)\left[F^{III}_{es} - B^{III}_{es}\right]\end{aligned} \tag{4}$$

$$T^{III}_{hr\to i,k} = A^{III}_r \frac{\cos\left(\frac{i\pi}{a}x\right)}{\sqrt{1+\delta_{0i}}}\frac{\cos\left(\frac{k\pi}{c}z\right)}{\sqrt{1+\delta_{0k}}}$$

$$T^{III}_{es\to m,n} = D^{III}_s \sin\left(\frac{i\pi}{a}x\right)\sin\left(\frac{k\pi}{c}z\right) \tag{5}$$

$$Z^{III}_{hr\to i,k} = \frac{1}{Y^{III}_{hr}} = \frac{\omega\mu_0}{\sqrt{k_0^2\varepsilon_r - \left(\frac{i\pi}{a}\right)^2 - \left(\frac{k\pi}{c}\right)^2}}$$

$$Y^{III}_{es\to i,k} = \frac{1}{Z^{III}_{es}} = \frac{\omega\varepsilon_0\varepsilon_r}{\sqrt{k_0^2\varepsilon_r - \left(\frac{i\pi}{a}\right)^2 - \left(\frac{k\pi}{c}\right)^2}} \tag{6}$$

The respective fields and quantities in region IV are taken as a superposition of those in regions I to II. Then the generalized scattering matrix of the three-port is obtained as follows. First, the transverse electric fields are matched at the boundaries with the respective other two ports shorted. This results in expressions for the wave amplitudes in region IV. Secondly, matching the transverse magnetic fields yields the overall scattering matrix of the junction. The reader is referred to [6] for details. The short and the end of region II is incorporated by using its input reflection coefficient at $z=c$ (Fig. 2):

$$\Gamma = Diag\left\{-exp\left(-j2k^{II}_{zq,p}L_s\right)\right\} \tag{7}$$

where k_z are the propagation constants in region II, and L_s is the distance between $z=c$ and the short. Assuming that the generalized scattering parameter submatrices of the junction are denoted by $S_{m,n}$ (m,n =1, 2, 3), then the two-port submatrices between ports I and III are:

$$\begin{aligned} S^{2p}_{11} &= S_{11} + S_{12}WS_{21} \qquad S^{2p}_{13} = S_{13} + S_{12}WS_{23} \\ S^{2p}_{31} &= S_{31} + S_{32}WS_{23} \qquad S^{2p}_{33} = S_{33} + S_{32}WS_{23} \end{aligned} \tag{8}$$

where $W = \Gamma\left(I - S_{22}\Gamma\right)^{-1}$ and I is the unity matrix.

Once this procedure is established, it can also be used to analyze the shorted waveguide junction between ports I' and II' by changing the dimensions and material constants accordingly.

Finally, the aperture of metallization thickness t is considered by a discontinuity that includes not only the aperture size but also a change in waveguide width as for the same frequency band, the waveguide is usually wider than the SIW due the lack of substrate material.

Waveguide apertures and resonators can now be added by standard MMT procedures [6].

III. Results

In order to verify the MMT code based on the theory presented in Section II, an SIW-to-SMW transition is designed for operation in the 19 GHz range. In order to create significant frequency sensitivity, a single TE_{10}-mode resonator is added to the top waveguide. Fig. 3 shows the top and side views of the structure clearly identifying the different layers, the coupling aperture, the resonator and the via holes in the SIW. For given SIW and waveguide widths, the initial size of the aperture, which acts as inverter to the waveguide resonator, is determined by filter theory, e.g. [7]. The final value as well as the exact positions of the SIW and waveguide shorts are determined by fine optimization within the MMT.

Fig. 4 shows the results obtained by the MMT and compares them to simulations in CST and HFSS. Very good agreement is observed in general. The only discrepancy appears to be a very slight frequency shift of 18 MHz which amounts to less than 0.1 percent at 19 GHz. The deviation is attributed to the fact that CST and HFSS simulate the actual via holes and the initial transition to an all-dielectric filled waveguide (Fig. 3, left). The MMT routine considers only the equivalent waveguide width of the SIW [5] in view of a simple and fast MMT implementation.

Initial test have shown that the MMT code, depending on implementation, is at least one order of magnitude faster than

CST and HFSS. Thus the extremely small deviation is acceptable in view of a timelier optimization and design process of SMW components.

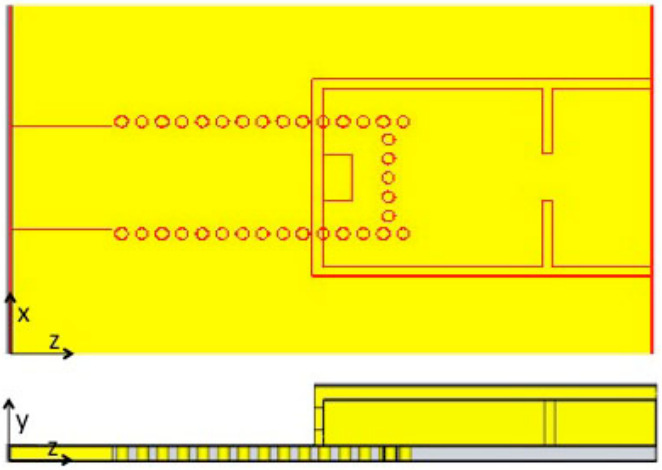

Fig. 3. Top and side views of the SIW-to-SMW transition with additional waveguide TE_{10}-mode resonator.

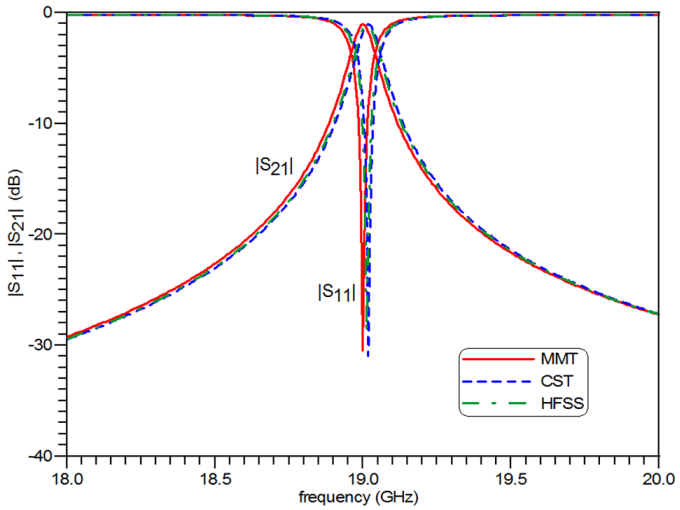

Fig. 4. Comparison of results obtained by the MMT with those of simulations in CST and HFSS.

IV. Conclusions

A mode-matching technique for the analysis and design of substrate mounted waveguide components on substrate integrated waveguide technology is presented. The method is rigorous and includes the metallization thickness of the aperture. The specific segmentation of discontinuities in the MMT permits the use of regular waveguide TE_{mn} and TM_{mn} modes. Results obtained for a single resonant structure, which consists of the SIW-to-SMW transition and an added waveguide TE_{10}-mode cavity, shows very good agreement with CST and HFSS simulations. It is expected that this technique will aid in the timely optimization and design of SMW components with the purpose of reducing losses in standard SIW filters and multiplexers.

Acknowledgement

The authors wish to acknowledge funding support for this work by the TELUS Research Grant in Wireless Communications.

References

[1] K. Wu, "State-of-the-art and future perspective of substrate integrated circuits (SICs)," Workshop Notes, *IEEE MTT-S Int. Microwave Symp.*, Anaheim, USA, May 2010.

[2] F. Taringou, J. Bornemann and K. Wu, "Broadband coplanar-waveguide and microstrip low-noise amplifier hybrid integrations for K-band substrate integrated waveguide applications on low-permittivity substrate," *IET Microw. Antennas Propag.*, vol. 8, pp. 99-103, Jan. 2014.

[3] W. Menzel and M. Wetzel, "Waveguide filter integrated into a planar circuit," *Proc. 32nd European Microwave Conf.*, pp. 957-960, Milan, Italy, Sep. 2002.

[4] T.J. Müller, W. Grabherr, and B. Adelseck, "Surface-mountable metalized plastic waveguide filter suitable for high volume production," *Proc. 33rd European Microwave Conf.*, pp. 1255-1258, Munich, Germany, Oct. 2003.

[5] Z. Kordiboroujeni and J. Bornemann, "Designing the width of substrate integrated waveguide structures," *IEEE Microw. Wireless Compon. Lett.*, vol. 23, pp. 518-520, Oct. 2013.

[6] J. Uher, J. Bornemann, and U. Rosenberg, *Waveguide Components for Antenna Feed Systems: Theory and CAD*, Norwood, MA: Artech House, 1993.

[7] G.L. Matthaei, L. Young, and E.M.T. Jones, *Microwave Filters, Impedance-Matching Networks, and Coupling Structures*, Dedham, MA: Artech House, 1980.